

**Controlling Susceptibilities of Quantum Dots Influenced by
Electromechanical Effects**

Prabhakar, S. and Melnik, R.

**Proceedings of the 2015 IEEE 35th International Conference on
Electronics and Nanotechnology (ELNANO),
ISBN 978-1-4673-6533-8, pp. 256-260, 2015.**

**2015 IEEE 35th International Conference on
ELECTRONICS AND NANOTECHNOLOGY
(ELNANO)**

**National Technical University of Ukraine
"Kyiv Polytechnic Institute"**

**CONFERENCE
PROCEEDINGS**

**April 21-24, 2015
Kyiv, Ukraine**

2015 IEEE 35th International Conference on Electronics and Nanotechnology (ELNANO)

**National Technical University of Ukraine
"Kyiv Polytechnic Institute"**

**Copyright © 2015 by the Institute of Electrical and Electronics Engineers, Inc.
All rights reserved.**

Copyright and Reprint Permission

Copyright and Reprint Permission: Abstracting is permitted with credit to the source. Libraries are permitted to photocopy beyond the limit of U.S. copyright law for private use of patrons those articles in this volume that carry a code at the bottom of the first page, provided the per-copy fee indicated in the code is paid through Copyright Clearance Center, 222 Rosewood Drive, Danvers, MA 01923. For reprint or republication permission, email to IEEE Copyrights Manager at pubs-permissions@ieee.org.

All rights reserved. Copyright©2015 by IEEE.

**IEEE Catalog Number: CFP1505U-USB
ISBN: 978-1-4673-6533-8**

Additional copies of this publication are available from
Organizing Committee of **ELNANO-2015**
Work phone: +38 (044) 454-90-65
E-mail: elnano@ieee.org.ua

Faculty of Electronics,
National Technical University of Ukraine "Kyiv Polytechnic Institute"
Polytekhnichna Str. 16/9, Block #12, off. 413-A,
03056, Kyiv, Ukraine

Controlling Susceptibilities of Quantum Dots Influenced by Electromechanical Effects

Sanjay Prabhakar, Roderick Melnik

MS2Discovery Interdisciplinary Research Institute,
M²NeT Laboratory, Wilfrid Laurier University,
75 University Ave West, Waterloo, ON, Canada L5C 4M5
rmelnik@wlu.ca, http://www.m2netlab.wlu.ca

Abstract – This contribution is devoted to the study of optical properties of AlN/GaN quantum dots, focusing on their susceptibility and electromechanical effects affecting such properties. We exemplify main ideas on a model based on the two-band strain-dependent Hamiltonian in cylindrical coordinates. On the first step of our procedure, the resulting strain-dependent two-band Hamiltonian model in effective mass approximation is solved for wurtzite AlN/GaN QDs numerically. Then the wavefunctions for three lowest levels, obtained from our first step, are employed to calculate the dipole moment matrix elements. Finally, the density matrix approach is used for calculation of susceptibility. The feasibility of controlling susceptibility is studied under the influence of electromechanical effects on quantum dot optical properties. Among other things, we demonstrate that electromechanical effects induce blue shifts in the resonance peak of susceptibility in wurtzite quantum dots under the study.

Keywords – quantum dots; optoelectromechanical properties, susceptibilities; coupled models; electromechanical effects; density matrix approach

I. INTRODUCTION

Wide band gap semiconductor materials such as AlN/GaN QDs have attracted significant attention due to their current and potential applications in optical, optoelectronic and electronic devices used in nano- and bionano- technological applications. Strongly coupled self-assembled QDs are grown either in the same wetting layer or a vertically stacked closely spaced layers. Single and vertically stacked double QDs grown by the Stranski-Krastanov process are of special interest because of their potential applications in QDs lasers, light emitting diodes, solar cells and other applications [1] – [10]. Strain is induced due to the lattice mismatch at the interfaces between two different types of semiconductors which can be used as a tuning parameter in tailoring the electronic and optical properties of single and multiple self assembled quantum dots [11] – [15]. Various approaches such as atomistic, pseudopotential and tight binding have been applied to investigate the optical and electronic properties of such nano-objects [7], [16] – [19].

On the other hand, resonance peaks observed in optical susceptibilities in devices made from semiconductor materials under the illumination of electromagnetic fields are of great interest for application in optoelectronic devices [20]. Optical susceptibilities in QDs are of great interest because QD

devices induce large dipole moments and strong responses to nonlinear optical interactions [20].

In this paper, we present a numerical analysis of band structures of single AlN/GaN QDs under the influence of electroelasticity. By using the Finite Element Method (FEM), we study the effect of electroelasticity on the electronic properties of truncated AlN/GaN QDs in the presence of wetting layers. Then, with the density matrix approach, we study the influence of electromechanical effects on the real and imaginary parts of linear susceptibility that corresponds to optical absorption and relative refractive index change. In particular, we show that the electromechanical effects induce blue shifts of the resonance peak in the linear susceptibility.

II. MATHEMATICAL MODEL FOR COUPLING CLASSICAL AND QUANTUM MECHANICAL PARTS

We start by writing the coupled equations of electromechanical effects of wurtzite structure cylindrical coordinates as [21]

$$\frac{\partial \sigma_{\rho\rho}}{\partial \rho} + \frac{\partial \sigma_{\rho z}}{\partial z} + \frac{\sigma_{\rho\rho} - \sigma_{\phi\phi}}{\rho} = 0, \quad (1)$$

$$\frac{\partial \sigma_{\rho z}}{\partial \rho} + \frac{\partial \sigma_{zz}}{\partial z} + \frac{1}{\rho} \sigma_{\rho z} = 0, \quad (2)$$

$$\frac{\partial D_{\rho}}{\partial \rho} + \frac{\partial D_z}{\partial z} + \frac{1}{\rho} D_{\rho} = 0. \quad (3)$$

The stress tensor components and the electric displacement vector components can be written as

$$\sigma_{\rho\rho} = C_{11}\epsilon_{\rho\rho} + C_{12}\epsilon_{\phi\phi} + C_{13}\epsilon_{zz} + e_{31}\partial_z V, \quad (4)$$

$$\sigma_{\phi\phi} = C_{11}\epsilon_{\phi\phi} + C_{12}\epsilon_{\rho\rho} + C_{13}\epsilon_{zz} + e_{31}\partial_z V, \quad (5)$$

$$\sigma_{\rho z} = 2C_{44}\epsilon_{\rho z} + e_{15}\partial_{\rho} V, \quad (6)$$

$$\sigma_{zz} = C_{13}\epsilon_{\rho\rho} + C_{13}\epsilon_{\phi\phi} + C_{33}\epsilon_{zz} + e_{33}\partial_z V, \quad (7)$$

$$D_\rho = 2e_{15}\varepsilon_{\rho z} - e_1\partial_\rho V, \quad (8)$$

$$D_z = e_{31}(\varepsilon_{rr} + \varepsilon_{\phi\phi})e_{33}\varepsilon_{zz} - e_3\partial_z V + P_z^{sp}, \quad (9)$$

where C_{kl} are the elastic moduli constants, e_{ij} are the piezoelectric constant, e_i are the permittivity constants, V is the piezoelectric potential and $E = -\frac{\partial V}{\partial z}$ is the built-in piezoelectric field. In what follows, we apply this theoretical foundation and present the total strain tensor, accounting for both the standard Cauchy strain and the internal strain due to lattice mismatch, that is

$$\varepsilon_{ij} = \varepsilon_{ij}^{(u)} + \varepsilon_{ij}^{(0)} \quad (10)$$

with the Cauchy strain and the internal strain components defined by

$$\begin{aligned} \varepsilon_{ij}^{(u)} &= (\partial_j u_i + \partial_i u_j)/2, \\ \varepsilon_{ij}^{(0)} &= (\delta_{ij} - \delta_{il}\delta_{jl})\varepsilon_a^* + \delta_{il}\delta_{jl}\varepsilon_c^*, \end{aligned} \quad (11)$$

respectively. In our case we have

$$\varepsilon_{\rho\rho} = \frac{\partial u_\rho}{\partial \rho} + \varepsilon_a^*, \quad \varepsilon_{zz} = \frac{\partial u_z}{\partial z} + \varepsilon_c^* \quad (12)$$

$$\varepsilon_{\phi\phi} = \frac{u_\rho}{\rho} + \varepsilon_a^*, \quad \varepsilon_{\rho z} = \frac{1}{2} \left(\frac{\partial u_\rho}{\partial z} + \frac{\partial u_z}{\partial \rho} \right). \quad (13)$$

Here $\varepsilon_a^* = \frac{a_m - a_{QD}}{a_m}$ and $\varepsilon_c^* = \frac{c_m - c_{QD}}{c_m}$ are the local intrinsic strains along a and c directions, respectively (which are non-zero in the dot and zero otherwise) [22], [23]. Also, a_m , c_m and a_{QD} , c_{QD} are the lattice constants of the matrix and the QD, respectively.

The total Hamiltonian for the conduction band electrons are written as:

$$H = H_0 + H_e^\varepsilon, \quad (14)$$

Here, H_e^ε is the strain dependent part of the kinetic energy of the electron and H_0 can be written as:

$$\begin{aligned} H_0 &= p_x \frac{1}{m_e^\perp} p_x + p_y \frac{1}{m_e^\perp} p_y + \\ &+ p_z \frac{1}{m_e^\parallel} p_z + E_c(r_e) + eV(r_e) \end{aligned} \quad (15)$$

The strain dependent part of the electron Hamiltonian in (14) can be written as

$$H_e^\varepsilon = a_c^\parallel(r)\varepsilon_{zz}(r) + a_c^\perp(r)[\varepsilon_{xx}(r) + \varepsilon_{yy}(r)], \quad (16)$$

where a_c^\parallel and a_c^\perp are the conduction band deformation potentials along the symmetric and perpendicular directions to the symmetric axis. In cylindrical coordinates, we can write

$$\varepsilon_{xx} + \varepsilon_{yy} = \frac{\partial u_\rho}{\partial \rho} + \frac{u_\rho}{\rho} + 2\varepsilon_a^*.$$

Because the total Hamiltonian (17) commutes with the z -projection of the total momentum operator, [24] the eigenfunctions of the total Hamiltonian operator H in (14) can be written as [24], [25], [26]

$$\psi_j(\rho, \phi, z) = e^{im\phi} f_j(\rho, z), \quad (17)$$

where m is an integer and indices j corresponds to the components of the wavefunction of the total Hamiltonian H . Thus we write H in cylindrical coordinates as:

$$\begin{aligned} H &= -\frac{\hbar^2}{2m_0} \left[\frac{1}{\rho} \frac{\partial}{\partial \rho} \rho \frac{\partial}{\partial \rho} + \frac{\partial}{\partial z} \frac{1}{m_e^\parallel} \frac{\partial}{\partial z} - \frac{1}{\rho^2} \frac{1}{m_e^\perp} m^2 \right] + \\ &+ eV + a_c^\parallel \varepsilon_{zz} + a_c^\perp \left(\frac{\partial u_r}{\partial r} + \frac{u_r}{r} + 2\varepsilon_a^* \right). \end{aligned} \quad (18)$$

The differential eigenvalue problem corresponding to Hamiltonian (18) was solved numerically to obtain the lowest few eigenvalues and eigenstates with respect to the various parameters of the system.

Next, we apply the Density Matrix approach. This is well known method for calculation of susceptibilities in different media [27]. It requires the laws of quantum mechanics to calculate the different orders of susceptibilities. In this formalism, the equation of motion for each component of density operator is given by:

$$\frac{\partial \rho_{nm}}{\partial t} = \frac{1}{i\hbar} [H, \rho]_{nm} - \gamma_{nm} (\rho_{nm} - \rho_{nm}^{(eq)}), \quad (19)$$

where $\tilde{H} = H + V_{em}(t)$ and $V_{em}(t) = -\mu \cdot E_{em}(t)$ represents the energy interaction of the QD with the externally applied radiation field $E_{em}(t)$. The second term on the right-hand side is a phenomenological damping term, which indicates that ρ_{nm} relaxes to its equilibrium value $\rho_{nm}^{(eq)}$ at rate γ_{nm} . We assume that the electric field incident normally onto the sample where AlN/GaN QDs are grown along the z -direction. Here $\mu = -ez$ denotes the electric dipole moment. After following the well-known mathematical procedure, the linear susceptibility for the three level system in a resonance case is given by [27]:

$$\begin{aligned} \chi^{(1)}(\omega) &= \frac{N}{e_0 \hbar} \left[\frac{M_{10} M_{01}}{\omega_{10} - \omega - i\gamma_{10}} + \frac{M_{10} M_{01}}{\omega_{10} - \omega + i\gamma_{10}} + \right. \\ &\left. + \frac{M_{20} M_{02}}{\omega_{20} - \omega - i\gamma_{20}} + \frac{M_{20} M_{02}}{\omega_{20} - \omega + i\gamma_{20}} \right] \end{aligned} \quad (20)$$

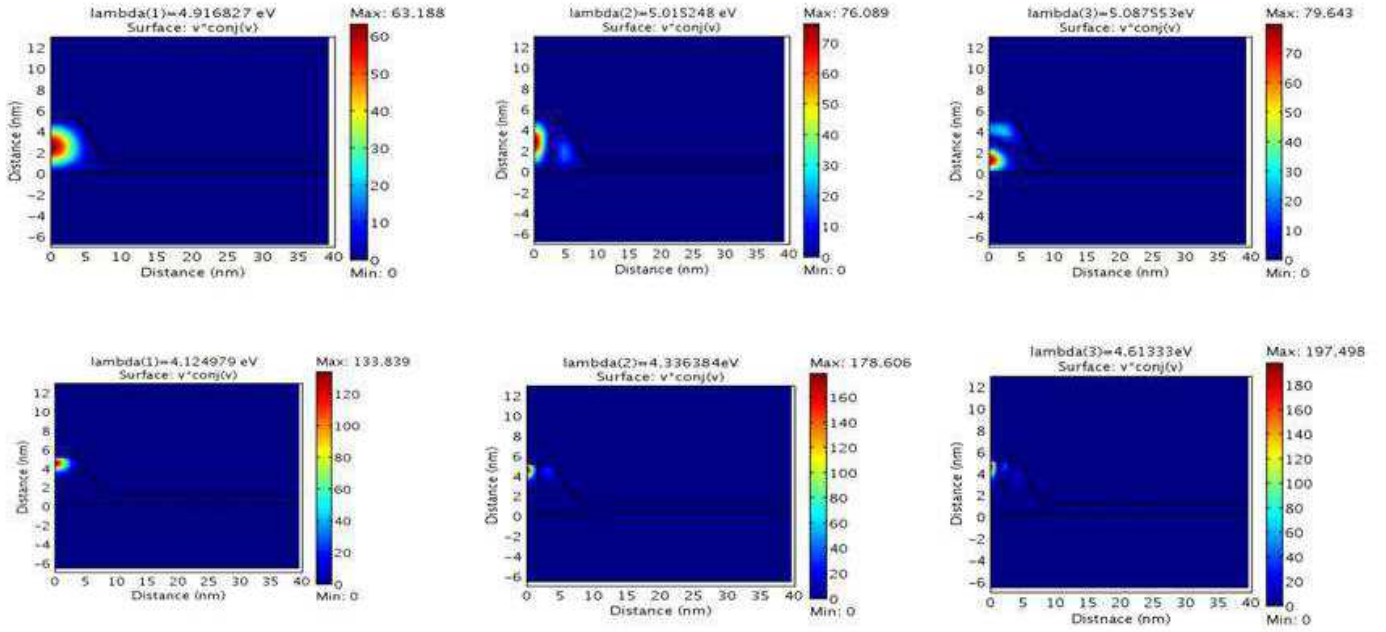


Fig. 1. The three lowest eigenvalues and wave functions of the electrons in the conduction band of AlN/GaN quantum dot without (upper panel) and with (lower panel) inclusion of piezoelectric effects.

where $M_{ij} = \langle \psi_i | e z | \psi_j \rangle$, $\omega_{ij} = (\varepsilon_f - \varepsilon_i)/\hbar$, ε_0 is the permittivity of free space and N is the carriers density. In the above, we assume that the main population of electrons in QDs lies in the ground state.

At the level of computational implementation of this new developed model, we use COMSOL based multiphysics finite element simulation strategy [28] to solve the corresponding eigenvalue PDE (Partial Differential Equation) problem with Schrödinger operator defined by the full Hamiltonian (14) which includes also the strain-dependent part (16), as explained above. We note here that the classical piezoelectric effect is linear. However, the model developed in this work can include also higher order nonlinear electromechanical effects too, as well as nonlinear strains. First attempts to incorporate systematically coupled effects with nonlinear strains into bandstructure models for quantum dots go to works [12] and [30]. The authors of [12] demonstrated that the application of linear models to the analysis of optoelectromechanical properties of nanostructures in bandstructure calculations may not always be adequate. Similar to [12], one of the approaches to generalize the developed here model would be to move from our Schrödinger-based PDE to the coupled Schrödinger-Poisson system where we can account consistently for the piezoelectric effect and analyze the influence of different nonlinear terms in strain components. Theoretical foundation on the inclusion of nonlinear strain effects in the Hamiltonian for nanoscale semiconductor structures and on a general treatment of deformation effects in Hamiltonians for inhomogeneous crystalline materials were developed in [29] and [30], respectively. In the latter work, the general method to treat Hamiltonians of deformed nanoscale systems was used to derive a second-order approximation both for the strong and

weak formulations of the eigenvalue problem. It was demonstrated that the weak formulation is needed in order to allow deformations that have discontinuous first derivatives at interfaces between different materials. As a matter of fact, as long as the deformation is twice differentiable away from interfaces, the weak formulation is equivalent to the strong formulation with appropriate interface boundary conditions. Moreover, because the Jacobian of the deformation appears in the weak formulation, the approximations of the weak formulation is not equivalent to the approximations of the strong formulation with interface boundary conditions. The developed theory provides a foundation upon which our generic approach has been based.

Another important issue to consider while generalizing the model developed here is to account for the influence of higher order nonlinear electromechanical effects. As it shown in [31] such influence can be quite important in a number of practically situations. The authors of [31] were the first to use a general three-dimensional axisymmetric coupled electromechanical model accounting for lattice mismatch, spontaneous polarization and higher-order nonlinear electrostriction effects in the application to the analysis of properties of quantum dots coupled with wetting layer. Notwithstanding that their generalized model that accounted for five independent electrostriction coefficients was efficiently solved numerically via a finite-element-method (FEM) implementation. The model (1)-(13) implemented here also via the FEM strategy can be extended to account for higher order nonlinear electromechanical effects in a way similar to [31]. Such effects are known to influence optoelectronic properties in bandstructure calculations based on a multiband effective mass theory. Bandstructure calculations in the context of susceptibility problems considered here can also be refined accordingly.

III. RESULTS AND DISCUSSIONS

We utilize a multi-physics simulation strategy based on the finite element method to provide a realistic description of the conduction band profile of AlN/GaN quantum dots with wetting layers with and without electromechanical effects, exemplifying our results on the piezoelectric effect. The idea is to solve the coupled equation of (1) through (3) in cylindrical coordinates to evaluate first the realistic piezoelectric effect contribution in quantum dots. Then, we solve the Schrödinger equation based on the Hamiltonian (18) without and with electromechanical effect contributions to get the wave functions and eigenvalues of the three lowest levels. In Fig. 1 (upper panel), we have plotted the three lowest levels of electron wave functions in quantum dots without electromechanical effects. Similarly, lower panel of Fig. 1 corresponds to the influence of piezoeffect contributions on the band structure of AlN/GaN quantum dots. As can be seen, the localization of electron wave functions is at the top of the quantum dots due to the influence of piezoeffect contributions which provides a blue shift of the resonance peak in the susceptibility plot of quantum dots under the illumination of electromagnetic fields (see Fig. 2). We have plotted the real and imaginary parts of the linear susceptibility vs frequency in Fig. 2. For the case without electromechanical effect (solid and dashed lines in Fig. 2), we find the resonance peaks at $\omega \approx 150 \text{ THz}$ and $\omega \approx 260 \text{ THz}$ which correspond to the transition of electron from first excited to ground states and from second excited to the ground states, respectively. Similarly, for the case with electromechanical effect (dotted and dashed dotted lines in Fig. 2), the resonance peaks at $\omega \approx 321 \text{ THz}$ and $\omega \approx 741 \text{ THz}$ correspond to the transition of electron from first excited to ground states and from second excited to the ground states, respectively. Comparing resonance peaks for two different cases (with and without electromechanical effects), we see that the resonance peaks are shifted to the higher frequency for the case of electromechanical effects in the band structure of wurtzite quantum dots which might provide the evidence of blue shifts of resonance peaks in quantum dots.

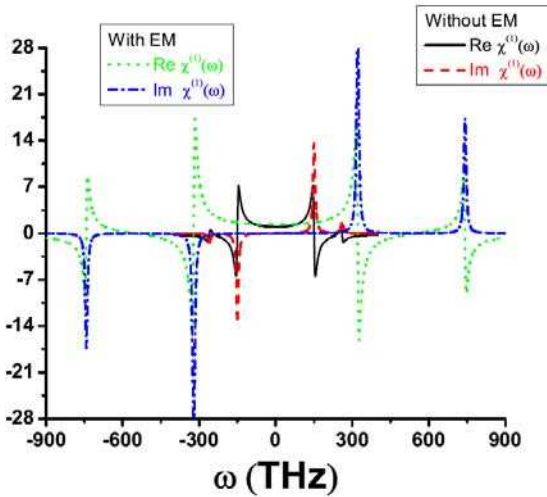


Fig. 2. Real and imaginary parts of the linear susceptibility. Here we chose $N = 10^{-18} \text{ cm}^{-3}$, $\gamma_{11} = \gamma_{22} = \gamma_{33} = 10 \text{ THz}$, $\gamma_{21} = \gamma_{31} = \gamma_{32} = 5 \text{ THz}$.

CONCLUSIONS

To conclude, we have shown that electromechanical effect contributions moved the localization of electron wavefunctions near the top of the dots. We have also shown that with and without piezoeffect contributions in quantum dots, the resonance peaks in the susceptibility can be observed at different frequencies. In particular, we have shown that the electromechanical effect contributions induce blue shifts of resonance peaks in the linear susceptibility of wurtzite quantum dots.

ACKNOWLEDGMENT

This work was supported by NSERC and CRC program.

REFERENCES

- [1] S. J. Pearton, C. R. Abernathy, M. E. Overberg, G. T. Thaler, D. P. Norton, N. Theodoropoulou, A. F. Hebard, Y. D. Park, F. Ren, J. Kim, and L. A. Boatner, "Wide band gap ferromagnetic semiconductors and oxides", *Journal of Applied Physics*, vol. 93, pp. 1–13, 2003.
- [2] W. Shan, T. J. Schmidt, X. H. Yang, S. J. Hwang, J. J. Song, and B. Goldenberg, "Temperature dependence of interband transitions in gan grown by metalorganic chemical vapor deposition," *Applied Physics Letters*, vol. 66, pp. 985–987, 1995.
- [3] B. Lin, Z. Fu, and Y. Jia, "Green luminescent center in undoped zinc oxide films deposited on silicon substrates," *Applied Physics Letters*, vol. 79, pp. 943–945, 2001.
- [4] A. Rubio, J. L. Corkill, M. L. Cohen, E. L. Shirley, and S. G. Louie, "Quasiparticle band structure of aln and gan," *Phys. Rev. B*, vol. 48, pp. 11810–11816, 1993.
- [5] Y. Kato, S. Kitamura, K. Hiramatsu, and N. Sawaki, "Selective growth of wurtzite GaN and AlGa_{0.15}N on GaN/sapphire substrates by metalorganic vapor phase epitaxy," *Journal of Crystal Growth*, vol. 144, pp. 133–140, 1994.
- [6] G. Yu, G. Wang, H. Ishikawa, M. Umeno, T. Soga, T. Egawa, J. Watanabe, and T. Jimbo, "Optical properties of wurtzite structure gan on sapphire around fundamental absorption edge (0.78 eV/4.77 eV) by spectroscopic ellipsometry and the optical transmission method," *Applied Physics Letters*, vol. 70, pp. 3209–3211, 1997.
- [7] S. H. Park and S. L. Chuang, "Piezoelectric effects on electrical and optical properties of wurtzite gan/algan quantum well lasers," *Applied Physics Letters*, vol. 72, pp. 3103–3105, 1998.
- [8] L. C. L. Y. Voon, C. Galeriu, B. Lassen, M. Willatzen, and R. Melnik, "Electronic structure of wurtzite quantum dots with cylindrical symmetry," *Applied Physics Letters*, vol. 87, 041906, 2005.
- [9] B. Daudin, F. Widmann, G. Feuillet, Y. Samson, M. Arlery, and J. L. Rouvière, "Stranski-Krastanov growth mode during the molecular beam epitaxy of highly strained gan," *Phys. Rev. B*, vol. 56, pp. R7069–R7072, 1997.
- [10] F. Widmann, J. Simon, B. Daudin, G. Feuillet, J. L. Rouvière, N. T. Pelekanos, and G. Fishman, "Blue-light emission from gan self-assembled quantum dots due to giant piezoelectric effect," *Phys. Rev. B*, vol. 58, pp. R15989–R15992, 1998.
- [11] S. R. Patil and R. V. N. Melnik, "Coupled electromechanical effects in II-VI group finite length semiconductor nanowires," *Journal of Physics D: Applied Physics*, vol. 42, 145113, 2009.
- [12] R. V. N. Melnik and R. Mahapatra, "Coupled effects in quantum dot nanostructures with nonlinear strain and bridging modelling scales," *Computers & Structures*, vol. 85, pp. 698 – 711, 2007.
- [13] S. R. Patil and R. V. N. Melnik, "Thermoelectromechanical effects in quantum dots," *Nanotechnology*, vol. 20, 125402, 2009.
- [14] R. V. N. Melnik and M. Willatzen, "Bandstructures of conical quantum dots with wetting layers," *Nanotechnology*, vol. 15, pp. 1–8, 2004.
- [15] R. V. N. Melnik and K. N. Zotsenko, "Finite element analysis of coupled electronic states in quantum dot nanostructures," *Modelling and*

- Simulation in Materials Science and Engineering, vol. 12, 465–477, 2004.
- [16] V. A. Fonoberov and A. A. Balandin, “Excitonic properties of strained wurtzite and zinc-blende GaN/Al_{0.25}Ga_{0.75}N quantum dots,” *Journal of Applied Physics*, vol. 94, pp. 7178–7186, 2003.
- [17] W. Jaskolski, M. Zielinski, G. W. Bryant, and J. Aizpurua, “Strain effects on the electronic structure of strongly coupled selfassembled InAs/GaAs quantum dots: Tight-binding approach,” *Phys. Rev. B*, vol. 74, 195339, 2006.
- [18] R. Santoprete, B. Koiller, R. B. Capaz, P. Kratzer, Q. K. K. Liu, and M. Scheffler, “Tight-binding study of the influence of the strain on the electronic properties of InAs/GaAs quantum dots,” *Phys. Rev. B*, vol. 68, 235311, 2003.
- [19] G. Bester, J. Shumway, and A. Zunger, “Theory of excitonic spectra and entanglement engineering in dot molecules,” *Phys. Rev. Lett.* vol. 93, 047401, 2004.
- [20] N. Suzuki and N. Iizuka, “Feasibility study on ultrafast nonlinear optical properties of 1.55μm intersubband transition in AlGaIn/GaN quantum wells,” *Jpn. J. Appl. Phys.*, vol. 36, L1006–L1008, 1997.
- [21] R. V. N. Melnik, “Generalised solutions, discrete models and energy estimates for a 2D problem of coupled field theory,” *Applied Mathematics and Computation*, vol. 107, 27–55, 2000.
- [22] S. Prabhakar and R. Melnik, “Influence of electromechanical effects and wetting layers on band structures of AlN/GaN quantum dots and spin control,” *Journal of Applied Physics*, vol. 108, 064330, 2010.
- [23] S. Prabhakar, R. Melnik, and L. L. Bonilla, “Coupled multiphysics, barrier localization, and critical radius effects in embedded nanowire superlattices,” *Journal of Applied Physics*, vol. 113, 244306, 2013.
- [24] E. Tsitsishvili, G. S. Lozano, and A. O. Gogolin, “Rashba coupling in quantum dots: An exact solution,” *Phys. Rev. B*, vol. 70, 115316, 2004.
- [25] J. Y. Fu and M. W. Wu, “Spin-orbit coupling in bulk ZnO and GaN,” *Journal of Applied Physics*, vol. 104, 093712, 2008.
- [26] W. H. Kuan, C. S. Tang, and W. Xu, “Energy levels of a parabolically confined quantum dot in the presence of spin-orbit interaction,” *Journal of Applied Physics*, vol. 95, pp. 6368–6373, 2004.
- [27] R. W. Boyd, *Nonlinear Optics*, 3rd ed., Academic Press: Burlington, 2008.
- [28] Comsol Multiphysics Reference Guide. Version 4.3a, 2012, Comsol, 750 pages.
- [29] B. Lassen, M. Willatzen, R. V. N. Melnik, L. C. Lew Yan Voon, “A General Treatment of Deformation Effects in Hamiltonians for Inhomogeneous Crystalline Materials,” *Journal of Mathematical Physics*, vol. 46, 112102, 2005.
- [30] B. Lassen, M. Willatzen, R. V. N. Melnik, “Inclusion of nonlinear strain effects in the Hamiltonian for nanoscale semiconductor structures,” *Journal of Computational and Theoretical Nanoscience*, vol. 3, 588–597, 2006.
- [31] M. Bahrami-Samani, S. R. Patil, R. Melnik, “Higher-order nonlinear electromechanical effects in wurtzite GaN/AlN quantum dots,” *Journal of Physics - Condensed Matter*, vol. 22, 495301, 2010.

Preparation and Some Properties of Pure and Doped Barium Titanate Thin Films	204
N. Korobova, S. Timoshenkov, E. Artemov, G. Kosolapova, V. Petrova	
Modeling of Stratified Graphene-Dielectric Structures Using the Generalized Boundary Conditions: THz Wave Scattering by a Thin Sandwiched Disk	207
Mikhail V. Balaban	
Wave Propagation Collapse in the Polariton Negative Dielectric Band of Crystal	211
S.G. Felinskyi, G. S. Felinskyi	
Nanostructured Sensors in Application to Computer-based Systems and Electronics	214
Klym H., Kochan R., Karbovnyk I.	
Hollow-Cathode Plasma-Assisted Atomic Layer Deposition: a Novel Route for Low-Temperature Synthesis of Crystalline III-Nitride Thin Films and Nanostructures	218
Necmi Biyikli, Cagla Ozgit-Akgun, Eda Goldenberg, Ali Haider, Seda Kizir, Tamer Uyar, Sami Bolat, Burak Tekcan, Ali Kemal Okayay	
Basic Equations of LEP for a Silver Strip Nanolaser	222
Olga V. Shapoval	
Elements for Photodetectors Based on Epitaxial Layers In_4Se_3, In_4Te_3 and Cdsb	225
George Vorobets, Olexandr Vorobets, Volodymyr Strebezhev, Viktor Strebezhev, Yuriy Khalavka, Vitaliy Balazyuk	
Analysis of the Modes of a Core-Shell Plasmonic Nanowire Laser with a Silver Core	228
Denys M. Natarov, Jiří Čtyroký	
Microwave Dielectric Measurement Methods on the Base of the Composite Dielectric Resonator	231
Tatarchuk D.D., Molchanov V.I., Pashkov V.M., Franchuk A.S.	
Microstrip Microwave Devices with Traveling Wave Resonator	235
Eduard Glushechenko	
Thermal Analysis of High-Power Multi-Finger FET	239
Vladimir Timofeyev, Elena Semenovskaya, Elena Faleeva	
Multi-Rate Clock-Data Recovery Solution in High Speed Serial Links	242
Melikyan Vazgen, Sahakyan Arthur, Shishmanyar Aram, Hekimyan Arsen	
Modeling, Fabrication and High Power Optical Characterization of Plasmonic Waveguides	245
A. Lavrinenko, O. Lysenko	
Modification of Silicon Surface for Solar Cells	249
Anatoly Druzhinin, Valeriy Yerokhov, Stepan Nichkalo, Yevhen Berezhanskyi	
Interrupted Mode of the Boundary Friction in the Model of Shear Melting with Asymmetric Potential	252
Iakov Lyashenko, Anton Zaskoka	
Controlling Susceptibilities of Quantum Dots Influenced by Electromechanical Effects	256
Sanjay Prabhakar, Roderick Melnik	
Electrical Characteristics of the Carbon Nanotube Field-Effect Transistors With Extended Contacts Obtained Within <i>ab-initio</i> Based Model	261
Artem Fediai, Dmitry A. Ryndyk, Gianaurelio Cuniberti	

SECTION II. BIOMEDICAL ELECTRONICS AND SIGNAL PROCESSING:

Parameter Optimization of the Single Channel Late Reverberation Suppression Technique	269
Arkadiy Prodeus	
Noninvasive Evaluation of Glucose Concentration in the Human Blood Based on Electrocardiograms	275
Anatolii A. Pulavskyi, Sergey S. Krivenko, Stanislaw A. Krivenko	
The System of Ultrasonic Diagnostics Using Phase Information of the Secondary Sound Field	278
Ogir A.S., Chemeris A.A., Tarapata V.V., Ogir E.A.	
Effect of Mechano-Chemical Processing in the Synthesis of Weakly Agglomerated Ferromagnetic $\text{La}_{1-x}\text{Sr}_x\text{MnO}_3$ Nanoparticles on their Properties	282
Y. Shlapa, S. Solopan, A. Belous	